JOURNAL OF SPACECRAFT AND ROCKETS
Vol. 53, No. 4, July-August 2016

Engineering Notes

Magnetohydrodynamic Flow Control of a Hypersonic Cruise Vehicle Based on AJAX Concept

R. Balasubramanian,* K. Anandhanarayanan,† R. Krishnamurthy,† and Debasis Chakraborty†
Defence Research and Development Laboratory, Hyderabad 500 058, India

DOI: 10.2514/1.A33573

I. Introduction

IN THE history of space exploration, rockets were the only flight vehicles available for transportation such as Earth orbital missions for placing satellites, interplanetary flights, and military missions such as Intermediate Range Ballistic Missiless and Intercontinental Ballistic Missile. Most of these rockets flew a oneway mission of transportation from Earth to the destination and, upon completion of the mission, were either lost in space or fell back to Earth as debris, and hence were nonrecoverable. The cost associated with launching these flight vehicles and the imposing technological challenges, though considered as highly mature as of the present day, were overwhelmingly large. The U.S. Space Shuttle of and the Russian Buran/Energiya were designed and operated as the only reusable flying missions that could make several sorties between the Earth and the flight to orbit [1]. However, huge operating and maintenance costs associated with each of these missions, and the inexorable reliability and safety issues, gradually shelved them as unacceptable due to the present-day design philosophy of "low-cost access to space." Hence, next-generation space exploration required a different class of flight vehicles that was required to be cost efficient and fully reusable. In this realm, the hypersonic airbreathing propulsion system based on a supersonic combustion ramjet (SCRAMJET) was envisaged as the key technology platform for possible realization of the reusable launch vehicle (RLV) in full mission mode, which could perform orbital flights similar to that of spacecraft flown by a rocket system, although with logistics akin to that of an airliner, as on a day-to-day basis [2].

Active flow control of hypersonic flight vehicles forms a crucial design requirement for hypersonic research and technology development. The futuristic RLV concepts, such as the hypersonic cruise vehicle (HSCV) based on the SCRAMJET engine, require complex active flow control techniques that use new multidisciplinary and evolutionary physical mechanisms, such as electromagnetic and plasma discharge flow control, right from launch phase to touchdown. Hence, there is a need and demand to develop a multidisciplinary numerical tool considering the pertinent multiphysics environment for addressing research and development needs, as well as for analysis of various hypersonic flow control problems.

A schematic of the hypersonic cruise vehicle configuration based on the RLV concept is shown in Fig. 1. At hypersonic speeds, since the angle of the nose oblique shock is narrow, the entire forebody can be used for compressing the air, and hence forms part of the scramjet engine intake. Due to this, the intake characteristics are strongly coupled to the forebody shape of the HSCV; hence, the forebody is highly design optimized to provide adequate air ram compression and mass capture at the inlet. The exhaust duct of the HSCV scramjet engine is shaped as a nozzle having a considerable length, and it forms part of the HSCV aftbody. The nozzle provides adequate expansion of the combusted gases, which in turn provides thrust to the vehicle. It can be observed that there is a tight coupling of airframe with the propulsion system, and the flight conditions influence the propulsive performance, which in turn affects the aerodynamic performance of the vehicle as a whole, and hence necessitates an integrated aeropropulsive design approach.

One of the main challenges encountered in the HSCV design is that an adequate mass flow rate should be captured at the inlet and the inlet should start. During offdesign flight conditions, the air mass captured by the air intake might drastically reduce, which can result in flameout and thrust loss.

To counter the technical challenges of the HSCV design, such as the subcritical air-intake mass flow rate, high forebody heat flux rates, active thermal management, onboard power generation, thrust augmentation, etc., Vladimir Freighstadt of the Leninetz Holding Company in Russia proposed a novel AJAX vehicle concept [3] in the late 1980s. The AJAX concept hypersonic cruise aircraft was proposed to fly in the mesosphere (50–80 km altitude range) and incorporated various novel technologies based on plasma generation, magnetohydrodynamics (MHD) flow control systems, MHD power generation for controlling and augmenting the hypersonic flow, as well as for thermal management schemes [4–6]. The concept was conceived to use the existing adverse hypersonic environment around the vehicle toward its advantage. The AJAX concept made extensive utilization of MHD-based flow control techniques, where the fluid that was preionized and made electrically conducting was easily manipulated by an externally applied magnetic field. Hence, the hypersonic flowfield could be easily modified for convenience, even at offdesign flight conditions, by application of a suitable magnetic field.

Due to the use of various onboard MHD subsystems, such as the MHD-controlled inlet or MHD generator and MHD accelerator, the hypersonic ramjet engine is referred to as the magnetoplasma chemical engine, or MPCE. The schematic of the AJAX concept HSCV [6,7] is shown in Fig. 2. It has a waverider type of forebody design, followed by a flat upper surface to the body end, and it houses the MPCE along the midsection of the lower surface. The MHD generator shown in the figure inhibits the mass flow rate by application of a suitable magnetic field, thereby generating electric current.

The hydrocarbon endothermic fuel is converted into the hydrogen-enriched mixture and fed into the plasma-stabilized combustor for thermochemical reaction, and it sets on the combustion process. The exhaust products of combusted gas when entering the nozzle region are further accelerated using the MHD accelerator for providing additional thrust. The power source for the MHD accelerator is drawn from the electricity produced by the MHD generator at the inlet.

Since the oncoming air is preionized at the nose region of the HSCV, the overall drag of the vehicle is also reduced significantly. The ionizer housed at the nose region is a microwave beam generator that gets its power supply from MHD generator. As adequate power is generated within the MPCE to solve the high-energy needs of the

Received 26 January 2016; revision received 5 May 2016; accepted for publication 16 May 2016; published online 24 June 2016.

*Directorate of Computational Dynamics; bals.cfd@gmail.com (Corresponding Author).
†Directorate of Computational Dynamics.

AJAX-concept-based HSCV, the power demands are smartly and efficiently resourced on board.

II. Forebody Shock-on-Cowl-Lip Condition for HSCV

The forebody of the HSCV at hypersonic speed generates a shock system through which the air mass is captured by intake, and it is necessary to ensure that the shock system converges onto the cowl lip of the air intake for the mass flow to be critical. Since the shape of the forebody is fixed and designed for a specific design flight condition, the shock-on-cowl-lip condition cannot be achieved at offdesign conditions, leading to either subcritical or supercritical operation. The shock-on-cowl-lip condition at offdesign operation shall be met by using the MHD flow control technique, as proposed in the AJAX concept. To demonstrate the effectiveness of MHD as a futuristic proof-of-concept flow control technique for the HSCV scramjet intake, the CERANS-MHD [8] code is applied for a typical HSCV forebody [9] with a scramjet air intake for various flight conditions with imposed magnetic fields. During offdesign conditions, the two possible forebody shock structures shall be envisaged, such as the shock spilled out of the intake and the shock ingested into the intake. By applying a suitable magnetic field, both the scenarios can be transformed to a critical operating condition, whereby the shock-on-cowl-lip condition shall be achieved.

In the present study, movement of the shock and its impingement on the intake duct wall due to application of a magnetic field have been demonstrated. In the present work, the numerical study of Damevin et al. [9] was extensively referred to for comparison of results. In [9], the governing unsteady ideal MHD equations were solved in generalized coordinates using a modified four-stage Runge–Kutta scheme augmented with a Davis–Yee symmetric total variation diminishing limiter, and a local time step was used to obtain the steady-state solution.

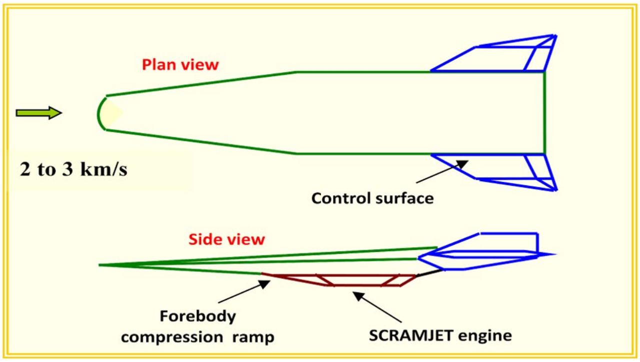

Fig. 1 Schematic of hypersonic scramjet cruise vehicle.

III. CERANS-MHD Code and Problem Description

The ideal MHD governing equations are implemented in the finite volume solver CERANS [10] (which stands for Compressible Euler/Reynolds Averaged Navier-Stokes with Magnetohydrodynamics, also called as CERANS-MHD [8,10]; they were validated for standard complex test cases available in the literature with very good comparative performance. The kinetic flux vector splitting scheme for MHD, by Xu [11], was used to model the advection terms. The divergence-free constraint for the magnetic field was ensured by Powell's eight-wave source term method [12]. The flow gradients were evaluated using the method of weighted least squares. Second-order spatial accuracy was obtained by using the procedure of reconstruction, and Barth's minimum–maximum limiter [13] is used to preserve monotonicity.

To demonstrate the effectiveness of MHD as a futuristic proof-of-concept flow control technique for the HSCV scramjet intake, the CERANS-MHD code was applied for a typical HSCV forebody [9] with a scramjet air intake.

IV. Computational Domain, Flow and Boundary Conditions

The schematic of the computational domain and the problem definition [9] are provided in Fig. 3. It shows the domain boundaries such as the far field, the compression ramp, the air-intake duct and outflow, the direction of freestream flow, the direction of imposed magnetic fields, the forebody oblique shock wave impingement, and its reflection on the intake duct. The grid consists of $211 \times 4 \times 181$ points along the length, into the plane of the paper, and below the compression ramp, respectively. The flow is assumed as two-dimensional, and since CERANS-MHD is a three-dimensional flow solver, it is necessary to include the spanwise direction with four points (three cells) into the plane of the paper for properly simulating the symmetry boundary conditions in the finite volume framework. The magnetic field is applied uniformly at an orientation of 45 deg with respect to the x axis (along the length), as indicated by the arrows in Fig. 3, and the values of x component and z component (vertical direction) magnetic fields are equal ($B_x = B_z$). The y component (spanwise direction) magnetic field value that lies into the plane of the paper is set to zero.

V. Results and Discussions

To study the effect of the magnetic field, a simulation is performed with a freestream Mach number of 10 and an altitude of 40 km, and the magnetic field strength is varied from $0T$ to $0.035T$ in steps of $0.007T$. The shock structures ahead of the air intake of the HSCV for the nonmagnetic case and for an imposed magnetic field of $0.035T$ are shown in Fig. 4 in the form of pressure contours. It can be observed that an oblique shock forms at the forebody compression ramp corner along with an expansion fan at the downstream junction of the compression ramp. Apart from these standard observations, an

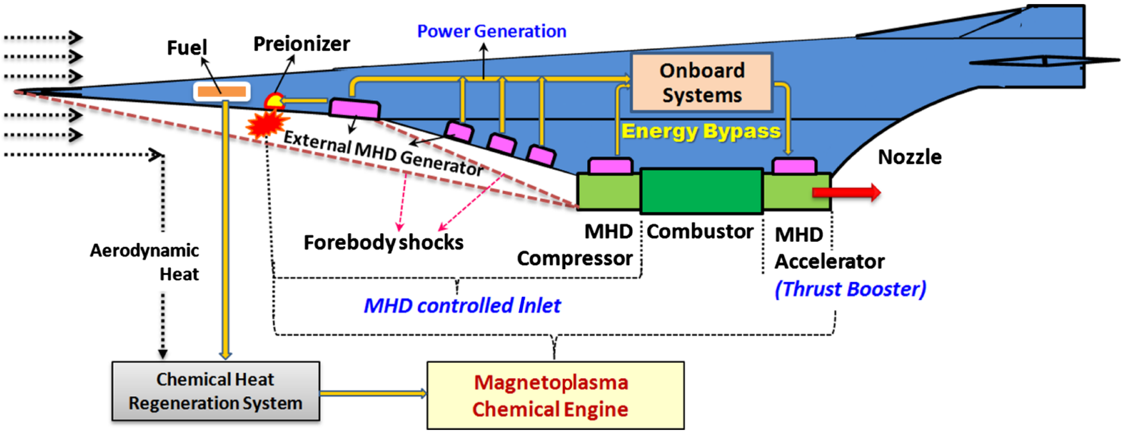

Fig. 2 AJAX concept hypersonic scramjet cruise vehicle [6,7].

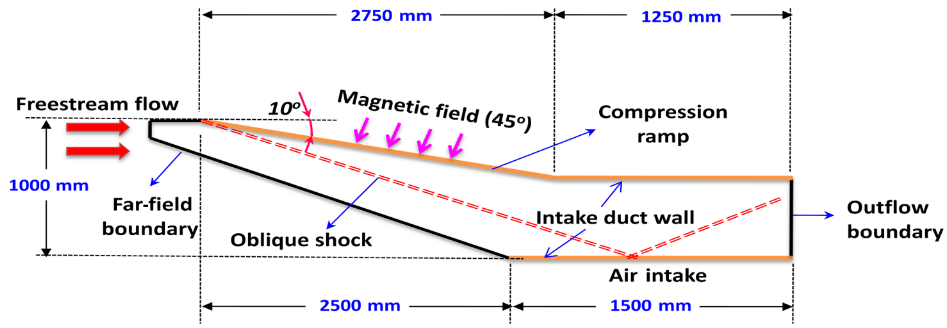

Fig. 3 Computational domain for MHD assisted air intake [9].

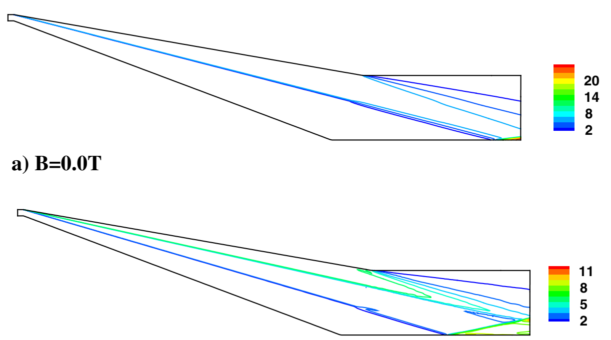

a) B=0.0T

b) B=0.035T

Fig. 4 Pressure contours, magnetic field variation study, Mach 10, and altitude of 40 km.

obvious distinguishing feature of that formation of a secondary compression wave between the oblique shock wave and the compression ramp is noticed. This feature is atypical in the inviscid nonmagnetic ($B = 0T$) flow simulation. The oblique shock interacts with the intake duct almost at the rear end of the computational domain for the inviscid simulations and gets reflected out of the computational domain.

As the magnetic field strength is increased, the shock moves upstream; hence, the oblique shock wave angle increases. Correspondingly, the shock impingement point keeps moving upstream. With an increase in magnetic field intensity, the strength of the secondary wave that starts to appear beyond the magnetic field of $0.014T$ also increases. For the imposed magnetic field value of $0.021T$ and beyond, the secondary wave is observed to interact with the reflected shock. This movement of shock due to application of the magnetic field clearly demonstrates the possibility of positioning the shock on the intake cowl lip for maximizing the air-mass capture.

The pressure profiles along the vertical (z axis) direction extracted at a downstream location of 1 m from the compression ramp corner are provided in Fig. 5. In this case, the z location of 0.55 m, which is at the lower end of the profile, corresponds to the far-field boundary and the z location of 0.823 m, which is at the top end of the profile, corresponding to the wall boundary of the compression ramp.

Various lines in the profile plot correspond to the CERANS-MHD simulations, and the various symbols correspond to data extracted from [9] for comparison. It can be observed that, as the magnetic field is increased, the wall pressure on the compression ramp decreases, which indicates an overall qualitative reduction in pressure drag. The formation of the secondary wave can be clearly noticed in the form of sudden discontinuities in the profiles, especially for magnetic fields from $0.014T$ to $0.035T$. It can be noted that, at lower magnetic field strengths, especially up to $0.014T$, the pressure jump due to the oblique shock is higher than the jump due to the secondary wave. In the case of a magnetic field of $0.021T$, the pressure jump due to the secondary wave is about 1.28, as against the oblique shock pressure jump of 4.41. For the $0.035T$ case, the pressure jump due to the secondary wave exceeds the jump due to oblique shock by about 29%. Hence, as the magnetic field increases, the strength of the secondary shock wave increases with respect to the forebody oblique shock, and this conclusion corroborates well with [9].

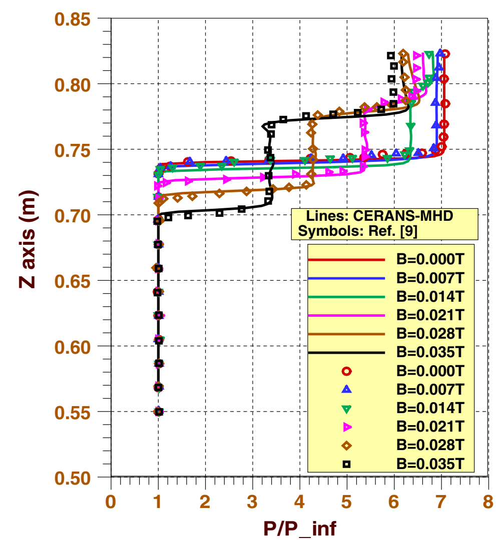

Fig. 5 Pressure profiles (p/p_∞) at $x = 1$ m from intake ramp of various magnetic fields.

Figure 6 depicts the wall pressure variation with an applied magnetic field at the downstream location of 1 m from the compression ramp corner. The trend and variation of the present simulation closely resemble the data of [9], and the maximum deviation between the two data is about 3.5%, occurring at the highest applied magnetic field of $0.035T$. It can be noted that, as the magnetic field is increased, the wall pressure decreases and the reduction is observed to be about 14% in the case of CERANS-MHD and about 18% due to [9] for the magnetic field variation from 0 to $0.035T$.

The variation of shock angle with magnetic field is shown in Fig. 7. It can be observed that the shock wave angle increases with the magnetic field and depicts a nonlinear variation. Also, the present simulation data have a very good quantitative agreement with the data of [9], which are higher by about 2% for the magnetic field of $0.035T$.

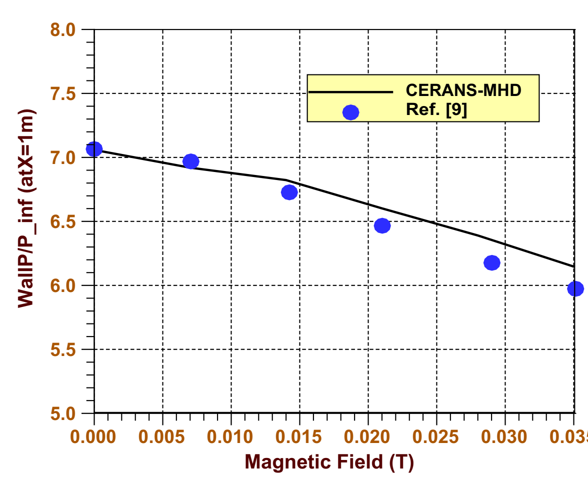

Fig. 6 Variation of wall pressure (p/p_∞) at 1 m location vs magnetic field.

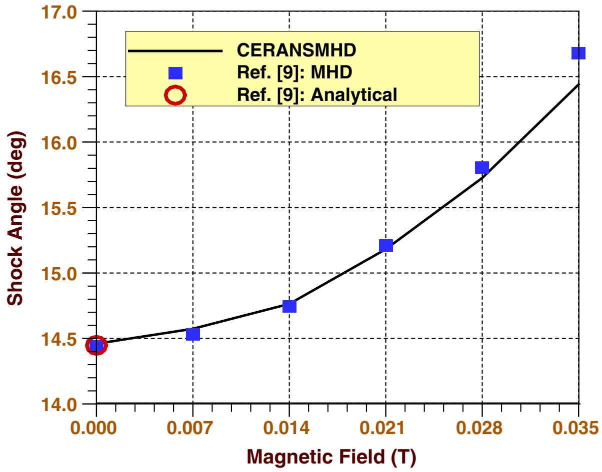

Fig. 7 Variation of shock angle vs magnetic field.

VI. Conclusions

The CERANS-MHD code is applied to demonstrate a proof-of-concept magnetohydrodynamic flow control technique for a hypersonic aerospace cruise vehicle based on the AJAX concept. Analyses are made by separately varying the applied magnetic field. It is demonstrated that the in-house-developed CERANS-MHD code is able to mimic the physical phenomenon associated with the interaction of the magnetic field with hypersonic flow. Due to application of the magnetic field, a secondary wave is observed to form between the oblique shock and the compression ramp of the forebody, thereby enabling the magnetic field to relocate the oblique shock, and hence the possibility of positioning the oblique shock on the cowl lip at offdesign flight conditions. A future course of study will consider resistive magnetohydrodynamics (MHD) modeling for including the effects of dissipative terms.

References

[1] Segal, C., *The Scramjet Engine Processes and Characteristics*, Cambridge Univ. Press, New York, 2009, pp. 12–13.

[2] McClinton, C. R., Rausch, V. L., Shaw, R. J., Mehta, U., and Naftel, C., "Hyper-X: Foundation for Future Hypersonic Launch Vehicles," *Acta Astronautica*, Vol. 57, Nos. 2–8, 2005, pp. 614–622. doi:10.1016/j.actaastro.2005.03.061

[3] Gurijnov, E. P., and Harsha, P. T., "AJAX: New Direction in Hypersonic Technology," *7th International Space Planes and Hypersonic Systems and Technologies Conference*, AIAA Paper 1996-4609, 1996.

[4] Van Wie, D. M., "Future Technologies—Application of Plasma Devices for Vehicle Systems," *Critical Technologies for Hypersonic Vehicle Development*, RTO AVT Lecture Series, von Kármán Inst. Rept. RTO-EN-AVT-116, Rhode-St-Genese, Belgium, 2004.

[5] Starikovskiy, A., and Aleksandrov, N., "Nonequilibrium Plasma Aerodynamics," *Aeronautics and Astronautics*, edited by Mulder, M., InTech, Rijeka, Croatia, 2011, Chap. 3, http://www.intechopen.com/books/aeronautics-and-astronautics/nonequilibrium-plasma-aerodynamics [retrieved 2016].

[6] Lee, Y.-M., Czysz, P. A., and Petley, D., "Magnetohydrodynamic Energy Bypass Applications for Single Stage-to-Orbit Vehicles," *10th International Space Planes and Hypersonic Systems and Technologies Conference*, AIAA Paper 2001-1901, 2001.

[7] Kuranov, A. L., Korabelnicov, A. V., Kuchinskiy, V. V., and Sheikin, E. G., "Fundamental Techniques of the "AJAX" Concept. Modern State of Research," *10th International Space Planes and Hypersonic Systems and Technologies Conference*, AIAA Paper 2001-1915, 2001.

[8] Balasubramanian, R., and Anandhanarayanan, K., "An Ideal Magnetohydrodynamics Solver for High Speed Flows," *Proceedings of the 16th Annual CFD Symposium*, Aeronautical Soc. of India Paper CP-05, Bangalore, India, Aug. 2014.

[9] Damevin, H.-M., Hoffmann, K. A., and Dietiker, J.-F., "Numerical Simulation of Hypersonic MHD Applications," *30th AIAA Plasmadynamics and Lasers Conference*, AIAA Paper 1999-3611, 1999.

[10] Balasubramanian, R., and Anandhanarayanan, K., "Higher Order Accurate Reconstruction Scheme for the Navier-Stokes Equations on Finite Volume Polyhedral Grids," *Proceedings of the Seventh Asian Computational Fluid Dynamics Conference, ACFD-7*, Aeronautical Soc. of India, Bangalore, India, Nov. 2007, pp. 875–883.

[11] Xu, K., "Gas-Kinetic Theory Based Flux Splitting Method for Ideal Magnetohydrodynamics," *Journal of Computational Physics*, Vol. 153, No. 2, 1999, pp. 334–352. doi:10.1006/jcph.1999.6280

[12] Powell, K. G., "An Approximate Riemann Solver for Magnetohydrodynamics (That Works in More than One Dimension)," Inst. for Computer Applications in Science and Engineering, TR-94-24, Langley, VA, 1994.

[13] Barth, T. J., and Jespersen, D. C., "The Design and Application of Upwind Schemes on Unstructured Meshes," *27th Aerospace Sciences Meeting*, AIAA-89-0366, 1989.

M. Miller
Associate Editor